Author version: *Cont. Shelf Res., vol.119; 2016; 30-39*

Spatial variability in phytoplankton community structure along the eastern Arabian Sea during the onset of south-west monsoon

Ayaz Ahmed, Siby Kurian, Mangesh Gauns*, Chndrasekhararao A.V, Amara Mulla,
Bhagyashri Naik, Hema Naik and S.W.A Naqvi
CSIR-National Institute of Oceanography, Dona Paula Goa-403004

*Corresponding author: Dr. Mangesh Gauns, e-mail gmangesh@nio.org

Abstract

The Arabian Sea experiences moderate to weak upwelling along the south-west coast of India, which subsequently propagates towards the north. This causes variation in plankton community composition, which is addressed in the present study. Here we report the spatial variations in distribution of phytoplankton groups along the north-south transect in the eastern Arabian Sea based on marker pigments supported with flow-cytometric and microscopic analyses. 15 phytoplankton pigments were identified using High-performance liquid chromatography (HPLC) and the chemotaxonomic software (CHEMTAX) analysis associated these to seven major group of phytoplankton. The phytoplankton biomass, chlorophyll *a* (Chl *a*) was higher in southern stations with dominance of fucoxanthin whereas, divinyl chlorophyll *a* (divinyl Chl *a*), marker pigment of *Prochlorococcus* was present only in the northern region. Microscopic observation revealed the dominance of larger forms; diatoms (*Chaetoceros coarctatum* and *Nitzschia* sp.) and dinoflagellates (*Scrippsiella* sp., *Oxytoxum nanum* and *Oxytoxum* sp.) in the southern region. Furthermore, a study of plankton size distribution showed dominance of picoplankton (f_{pico}) followed by nanoplankton (f_{nano}) along the northern stations with comparatively higher microplankton (f_{micro}) in the south. This study clearly showed the influence of different environmental conditions on the phytoplankton community as reflected in dominance of diatoms in the southern (south of 12 °N) and that of picoplankton in the northern (north of 12 °N) region.

Keywords: Phytoplankton pigments, Picoplankton, CHEMTAX, Eastern Arabian Sea

1. Introduction

The Arabian Sea is one of the five major upwelling zones of the world ocean. Upwelling that occurs in the region is most vigorous along the western boundary (Somalia-Arabia coast) compared to the eastern part along the south-west coast of India (Banse, 1959;1968). However this process is restricted to the south-west monsoon (SWM, June to September), but because of the vigorous circulation during this season it affects a very large area where nutrient rich subsurface water is brought to the surface enhancing biological production (Banse, 1968; 1987; Sankaranarayanan et al., 1978; Naqvi et al., 2000; Wiggert et al., 2005; Habeebrehman et al., 2008). The resultant overall high productivity may contribute to the oxygen deficient condition along the western Indian shelf (Naqvi et al., 2000). Accounting for approximately one fourth of all plants in the world (Hallegraeaff and Jaffrey, 1985), marine phytoplankton are important contributors to global carbon fluxes (Falkowski et al., 1998). Phytoplankton in the ocean are composed of various taxonomic groups which together determine total production and their interaction at different trophic levels and also the flux of particulate carbon from the euphotic zone (Michaels and Silver, 1988; Peinert et al., 1989; Buesseler, 1998).

The Arabian Sea displays distinct oscillation patterns in phytoplankton biomass, which are linked to seasonal variations in atmospheric forcing and a strong coupling between the prevailing physical conditions and the biological processes (Banse, 1987; Brock and McClain, 1992; Brock et al., 1991; 1993; 1994). The combination of a wide range of physical conditions and warm water temperatures throughout the year results in highly diverse phytoplankton communities in the Arabian Sea (Simonsen, 1974; Taylor, 1976; Kleinje, 1991). Phytoplankton community structure in the Arabian Sea is therefore highly dependent upon prevailing environmental conditions, and diatoms are usually a significant component in the nutrient-rich upwelled waters during summer (Krey, 1973).

The present study attempts to characterize the phytoplankton community structure along a north-south (NS) transect in the near shore regions of the west coast of India. This study was carried out during the onset of south-west monsoon, when upwelling just begins along the southern coast of India. Here, we aim to understand the linkage between phytoplankton and environmental parameters prevailing in the study region.

2. Materials and methods

2.1. Study area and water sampling

This study was conducted during the 294th cruise of *ORV Sagar Kanya* (25th May to 26th June 2012). One set of 19 stations placed at 0.5° intervals in a transect (NS transect) parallel to the coast between

8 °N and 17 °N and another one with 6 stations perpendicular to the coast (Off Trivandrum, TVM transect) at 8.6 °N (Fig. 1) were occupied. Depths ranged between 600 and 800 m over the stations in the meridional transect and between 50 and 1250 m in the zonal transect.

At every station, profiles of water temperature, salinity, dissolved oxygen (DO) and fluorescence were obtained with a Sea-Bird Electronics (SBE) 9plus CTD unit equipped with pre-calibrated sensors for DO (SBE 43) and fluorescence (Seapoint). In addition, water samples were collected with 10 L Niskin samplers from two depths (surface and a depth of sub-surface chlorophyll maximum - Chl_{max}) and processed following JGOFS protocols (Knap et al., 1994) for chemical (nutrients) and biological (phytoplankton species composition and biomass as chlorophyll *a*) properties. The depth of Chl_{max} generally coincided with those of nutricline and of less-oxygenated waters.

2.1. Chemical measurements

Subsamples for nutrients were frozen on board at -20 °C and later analyzed in the shore laboratory for nitrate, phosphate and silicate in a Skalar auto analyzer following the methods given by Grasshoff et al. (1983).

2.3. Biological measurements

2.3.1. Phytoplankton cell counts (>10 µm)

A sub-sample of 250 ml was fixed with 2% Lugol′s iodine. All such samples were stored in the dark at room temperature until enumeration. A settling and siphoning procedure was followed to concentrate the samples which were then examined microscopically in a Sedgewick-Rafter plankton counting chamber (Structure Probe, Inc., West Chester, PA, USA) at ×200 magnification.

2.3.2. Picophytoplankton biomass

Water samples for picophytoplankton were fixed in glutaraldehyde (0.2% final concentration), quick-frozen in liquid nitrogen and stored at -80 °C until analysis. The analyses were carried out in a BD FACS Calibur Flow cytometer equipped with blue (488nm) and red lasers (633nm), and absolute counts were obtained following the procedure of Marie et al. (1997). A combination of FSC (forward scatter), SSC (side scatter), SSC-FL3 (red fluorescence) and FL2 (orange fluorescence)-FL3 plots was used to differentiate populations in the sample (Casamayor et al., 2007). 1 micron Fluoresbrite YG beads (Polysciences, Warrington, PA) were used as internal standards. The data were analyzed in CYTOPC software (Vaulot, 1989; 1990).

2.3.3. HPLC pigments

Water samples meant for the analysis of phytoplankton pigments were collected in amber-colored bottles and filtered (0.5 to 1 L) through Whatman GF/F filters (pore size 0.7 μm) in dark and stored at -80 °C until the analysis. The frozen filters were extracted at 0°C for 1-2 minutes in 3 ml of 100% methanol using Fisher Scientific ultrasonic dismembrator at 23 kHz. The methanol extracts were filtered using a Teflon syringe cartridge (pore size 0.45 μm) to remove cellular debris and analyzed using HPLC (Agilent Technologies) using an Eclipse XDB C8 column. Pigments were separated following the procedure as given in Roy et al. (2006) and Kurian et al. (2012) using gradient program and pigments were detected at 450 and 665 nm (Soret and Q-bands) by the diode array detector. Commercially available standards obtained from DHI Inc. (Denmark) were used for the identification and quantification of pigments including both chlorophylls and carotenoids. Identification was done based on the retention time and visible spectra matching.

2.3.4. CHEMTAX and phytoplankton size class analyses

Pigments such as fucoxanthin, peridinin, chlorophyll *b*, zeaxanthin and alloxanthin etc. are diagnostic of specific phytoplankton functional groups (diatoms, dinoflagellates, chlorophytes, cyanobacteria and cryptophytes respectively) (Table 1) and thus are useful in determining phytoplankton species-specific composition (Suzuki et al*.,* 1997; Jeffrey and Vesk, 1997; Barlow et al., 1998; Paerl et al., 2003; Barlow et al., 2008). The pigment composition obtained with HPLC as above hence was subjected to an analysis with CHEMTAX (chemical taxonomy) software (Mackey et al., 1996; Wright et al., 1996, 2009, 2010) to determine relative abundance and contribution of phytoplankton functional groups. CHEMTAX uses a factor analysis and steepest-descent algorithm to find the best fit of the data to an initial pigment ratio matrix. Initial pigment ratios for major algal classes were obtained from the literature (Gibb et al., 2001; Schluteret al., 2000, 2011). Based on the diagnostic pigments detected, 8 algal groups - prasinophytes, dinoflagellates, chlorophytes, cyanobacteria, diatoms, haptophytes, cryptophytes and chrysophytes - were loaded to CHEMTAX. The

$$f\_micro = \{1.41[fuco] + 1.41[perid]\}$$

$$f\_nano = \{1.27[19'HF] + 0.35[19'BF] + 0.60[Allo]\}$$

$$f\_pico = \{1.01[Chl\ b] + 0.86[Zea]\}$$

CHEMTAX input ratio was optimized based on Wright et al. (2009) and the output with the smallest residual was selected. The optimized pigment ratio of the matrix derived by CHEMTAX is presented in supplementary tables (Table S1.A and S1.B). Concentrations of different marker pigments were used to reconstruct the proportion of various phytoplankton size classes. The concentrations of chlorophyll *a* associated with each of the three phytoplankton classes (f_{micro}, f_{nano} and f_{pico}) were calculated following the equations as given below (Vidussiet al., 2001 and Uitzet al., 2006).

3. Results

3.1. Hydrographic and biogeochemical variations

3.1.1. *NS transect*

Latitudinal variations in temperature, salinity, dissolved oxygen and fluorescence are shown in Figure 2. Based on the hydrographic conditions, it was evident that the upwelling was prominent south of 12°N and accordingly the sampling stations were divided into two sections, northern (stations 1 to 12) and southern (stations 13 to 19). The surface water was warmer (sea surface temperature, SST: 28.5 - 29.7 °C) and more saline (sea surface salinity SSS: 34.1 - 36.1 psu) in the northern section than in the southern one (SST: 27 - 28.6 °C and SSS: 34 - 35.9 psu). In contrast, dissolved oxygen showed comparable values at the surface between northern (2.5- 4.1 ml L^{-1}) and southern (2.8 to 4.1 ml L^{-1}) sections. However, Figure 2 clearly shows shoaling of isolines

(temperature and DO) in the euphotic zone towards the southern section, which supported larger phytoplankton biomass as represented by fluorescence in the water column.

The concentrations of nitrate, phosphate and silicate in the surface waters did not show large variation between the northern and southern sections (Fig. 3A). However, as evident from the hydrographic parameters, the upwelled waters in the south displayed considerable buildup of nitrate and silicate at the depth of Chl_{max} (Fig. 3B). The values of nitrate, phosphate and silicate at this depth varied in the range of 0.1 - 4.8 µM, 0.23 - 0.59 µM and 2.13 - 3.87 µM respectively at northern stations but were higher at the southern stations (0.2 - 13.47 µM, 0.3 - 1.2 µM and 1.9 - 9.8 µM). In addition, colder (SST: 25.8 - 27.9 °C), low-oxygenated (1.7 - 4 ml L^{-1}) and nutrient-enriched (NO_3: 0.7 - 19.8 µM; PO_4: 0.36 - 1.48 µM and SiO_4:1.7 - 15.1 µM) waters were observed at the depth of Chl_{max} along TVM transect signifying upwelling.

3.2. Biological measurements

3.2.1. *NS transect*

The distribution of chlorophyll *a* showed large spatial variations along the NS transect during the onset of south-west monsoon. The Chl *a* concentrations in the surface waters were lower (131 - 1233 ng L^{-1}) than at Chl_{max} (191 - 1401 ng L^{-1}; Fig. 4A and 4B). Chl_{max} was generally present within a depth range of 10-50 m.

The concentrations of phytoplankton accessory pigments also varied between transects both at the surface and at Chl_{max} (Fig. 4A and 4B) with high diversity at the latter one. The concentrations (max. ng L^{-1}) of 19'HF (132), divinyl Chl *a* (118), zeaxanthin (116) and Chl *b* (68) were higher in surface water in the northern section whereas zeaxanthin (343), 19'HF (267), fucoxanthin (183), diadinoxanthin (73) and Chl *b* (69) were major contributors with higher concentrations in the south. Divinyl Chl *a* (120 ng L^{-1}), 19'HF (114), zeaxanthin (104) and 19' BF (50 ng L^{-1}) were the dominant marker pigments at the Chl_{max} in the northern stations. On the other hand, the accessory pigments in southern stations were dominated by 19' HF (max. 256 ng L^{-1}), zeaxanthin (211), fucoxanthin (186) and Chl *b* (176). In general, fucoxanthin and diadinoxanthin were in low concentrations in the north whereas divinyl Chl *a* was absent at most of the southern stations except at stations 13 and 19 where they were present in low concentrations.

3.2.2. *TVM transect*

Significant progression of upwelling was seen along the transect as reflected in the increased phytoplankton biomass (Chl *a*). Chl *a* concentrations in the surface water varied in the range of 314 - 5244 ng L^{-1} and between 347 and 4400 ng L^{-1} at Chl_{max}. Higher concentrations were recorded at

stations T3 and T4 (Fig. 5A and 5B). Accessory pigments (ng L^{-1}) in surface waters and at Chl_{max} were associated with the dominance of fucoxanthin (44 - 2481), zeaxanthin (28 - 506) and diadinoxanthin (13 - 175) (Fig. 5A and 5B).

3.3. Variation in relative pigments of phytoplankton size fractions

3.3.1. *NS transect*

Phytoplankton size fractions (f_{micro}, f_{nano} and f_{pico}) based on the concentrations of accessory pigments were derived to understand the variations of different communities along the transect. The concentrations of accessory pigments of f_{micro}, f_{nano} and f_{pico} in surface waters varied in the range of 4 - 30, 25 - 184 and 47 - 119 ng L^{-1} in the northern section but were much higher (8 - 268, 23 - 371 and 79 - 333 ng L^{-1}) in the southern section. Concentrations in the similar ranges were also observed at the Chl_{max} (Fig. 6A and 6B). The percentage contribution of microplankton was higher (avg. 32 %) in the southern section compared with the north (10 %), where nano- (42 %) and pico- (48 %) plankton were dominant.

3.3.2. *TVM transect*

The concentration (ng L^{-1}) of f_{micro}, f_{nano} and f_{pico} in the surface waters varied in the range 65 - 3509, 62 - 164 and 56 - 488, respectively. Concentrations in a range similar to that in the surface water were also observed at the $Chl_{max.}$ (Fig. 7A and 7B). Microplankton fraction contributed maximum biomass with an average contribution of 73% to the total accessory pigments, followed by picoplankton (14 %) and nanoplankton (13 %) along this transect.

3.4. CHEMTAX derived phytoplankton functional groups

3.4.1. *NS transect*

Relative contributions of various phytoplankton functional groups to the total Chl *a* was analyzed by CHEMTAX software which identified eight groups (chrysophytes, cryptophytes, haptophytes, diatoms, cyanobacteria, chlorophytes, dinoflagellates and prasinophytes). The concentration of Chl *a* associated with diatom assemblage was higher (101 to 636 ng L^{-1}: surface and 7 to 714 ng L^{-1}: Chl_{max}) in the southern section followed by cyanobacteria (up to 300 ng L^{-1}: surface) [Fig. 8A and B]. Cryptophytes also contributed significantly (up to 330 ng L^{-1}) in the southern than in the northern section (0.5 to 54 ng L^{-1}).

3.4.2. *TVM transect*

Relative Chl *a* associated with diatoms showed a major contribution along the TVM transect with higher concentrations (3194 ng L^{-1}: surface and 2703 ng L^{-1}: Chl_{max}) at station T3 (station depth: 300

m). These concentrations were much higher than those of cryptophytes (surface: 1163 ng L^{-1}; Chl_{max}: 1084 ng L^{-1}, Fig. 9A and 9B).

3.5. Phytoplankton cell count (>10 µm)

3.5.1. *NS transect*

Microscopic observation revealed the presence of diatoms and dinoflagellates with species counts of 23 and 29. Quantitatively, the dinoflagellates were dominant in the northern section at surface (0.7 to 2.7×10^3 cells L^{-1}) as well as at Chl_{max} (0 to 9.2×10^3 cells L^{-1}) and were dominated by species of *Scrippsiella* and *Oxytoxum.* The diatoms (the second major group) varied in the range of 1.3 to 2.4×10^3 cells L^{-1} at surface and 0.9 to 2.2×10^3 cells L^{-1} at Chl_{max}. The southern section, on the other hand, was dominated by diatoms (0 to 2.5×10^3 cells L^{-1} at surface and 0.96 to 10.66×10^3 cells L^{-1} at Chl_{max}). *Chaetoceros coarctatum* and *Nitzschia sp* were the most predominant forms.

3.5.2. *TVM transect*

The phytoplankton cell numbers were also higher along the TVM transect with maximum at T4 (station depth: 370 m). Diatoms formed a major assemblage of the phytoplankton with cell numbers varying from 1.6 to 466.7×10^3 cells L^{-1} at surface and 1.5 to 1108×10^3 cells L^{-1} at Chl_{max}. The major contributors in the diatom assemblages were *Dactyliosolen fragilissimus*, *Leptocylindrus danicus* and *Pseudo-nitzschia heimii.* Dinoflagellates were least represented in the transect with cell numbers ranging from 0 to 20×10^3 cells L^{-1} at surface and 0.5 to 3.1×10^3 cells L^{-1} at Chl_{max}.

To compare the phytoplankton species composition along the NS transect, one representative station of each section (stn. 6 from northern and stn.15 from southern) and a station (stn. T3) in the TVM transect are presented in Table 2. Diatom species *Dactyliosolen fragilissimus* showed dominance in the southern section including TVM transect whereas dinoflagellates were abundant at stn. 6 in the northern section with dominance of *Oxytoxum nanum* and *Scrippsiella* sp.

3.6. Picoplankton density

3.6.1. *NS transect*

Picoplankton were comprised of two major groups, *Synechococcus* and *Prochlorococcus,* with least contribution of picoeukaryotic algae (Fig. 10). *Synechococcus* was the major contributor of picoplankton biomass in both northern and southern sections. However, their cell numbers were higher in the southern section (surface: 2.02 to 10.4×10^7 cells L^{-1}, Chl_{max}: 0.24 to 5×10^7 cells L^{-1}) compared with the northern section (surface: 0.18 to 1.6×10^7 cells L^{-1}; Chl_{max}: 0.04 to 1.15×10^7 cells L^{-l}). *Prochlorococcus* abundance, on the other hand, was much higher in the northern section

(surface: 0 to 1.6×10^7 cells L^{-1} and Chl_{max}: 0.45 to 1.24×10^7 cells L^{-1}) than in the southern section (Chl_{max}: 0 to 0.4×10^7 cells L^{-1}, Fig. 6A and 6B).

3.6.2. *TVM transect*

Similar to NS transect, higher abundance of *Synechococcus* in surface water (0.6 to 8.2×10^7 cells L^{-1}) and at Chl_{max} (0 to 13.43×10^7 cells L^{-1}) was observed with a maxima at station T3. *Prochlorococcus* were present only at Chl_{max} with very low abundance (0 to 0.36×10^7 cells L^{-1}) [Fig. 7A and 7B].

4. Discussion

Coastal upwelling is a seasonal phenomenon along the west coast of India that begins in the southern region as early as May and propagates northward until November-December (Banse, 1959; Banse, 1968). Comparatively cooler upper water column with low salinity, dissolved oxygen content and high nutrients in the southern section (south of 12 °N) reflected progression of upwelling (Fig. 2 and 3) in the present study, as reported earlier by Shetye et al. (1990) and Naqvi et al. (2000). Concomitant spatial and seasonal variability in planktonic forms associated with upwelling has been reported previously from the region (Bhattathiri et al., 1996; Gauns et al., 1996; Ramaiah et al., 1996; Sawant and Madhupratap, 1996; Madhupratap et al*.,* 1996; Roy et al., 2006). However, information on picoplankton associated with the contrasting biogeochemical settings along the Eastern Arabian Sea is lacking.

Here we report phytoplankton composition based on HPLC technique (Wright and Jeffrey, 2006) supported by microscopic and flow cytometric analysis (Latasa and Bidigare, 1998). Among the accessory pigments, zeaxanthin, 19'HF and Chl *b* were present in higher concentration in surface waters and at Chl_{max} throughout the NS transect. However, distinct increase in total Chl *a* and fucoxanthin was seen both at surface and at Chl_{max} in the southern section (Fig. 4A and 4B). This was confirmed by microscopic analysis, which showed predominance of *Chaetoceros coarctatum, Nitzschia* sp*., Dactyliosolen fragilissimus, Thalassiosira* sp. and *Pseudonitzschia heinii*. These dominant diatoms have also been reported previously by Sawant and Madhupratap (1996), Roy et al. (2006) and Habeebrehman et al. (2008). The present study also complements previous reports addressing dominance of diatom in the upwelling systems (Cushing, 1989; Garrison et al., 1998; Brown et al., 1999; Menon et al., 2000; Jyothibabu et al., 2006).

During the onset of SW monsoon, the southern region remains productive where water in the euphotic zone becomes progressively replaced with nutrient rich waters in space and time following the upwelling. High concentrations of nitrate, phosphate and silicate (reaching up to ~14µM, ~1µM and ~10µM respectively - Fig. 3B) at Chl_{max} indicates a nutrient-rich water mass rising from deeper

depths and supporting particularly the microplankton (diatom) population. Dominance of diatoms as evident from both microscopic and HPLC analyses possibly led to decreased levels of silicate in the surface waters.

Picoplankton community was generally dominated by two groups, prochlorophytes (*Prochlorococcus*) and *Synechococcus,* common in tropical oceans and most likely representing systems associated with regenerated production (Claustre, 1994; Roy et al., 1996). These groups showed a distinct distribution patterns along the eastern Arabian Sea with the presence of *Prochlorococcus* in the northern section (max. at stn. 12 contributing ~ 39%) and dominance of *Synechococcus* in the southern section (Fig. 6A and 6B). This spatial variation possibly followed the trend previously observed elsewhere in eutrophic and oligotrophic waters (Campbell et al., 1997; Partensky et al., 1999; Durand et al., 2001; Sherr et al., 2005; Zwirglmaier et al., 2008). *Synechococcus* was associated with the surface waters with high concentrations of nitrogenous nutrients. On the other hand, northern section with lower nutrient concentrations in the upper water column favored the dominance of *Prochlorococcus* as reported by Campbell et al. (1998). Generally, smaller cells (picoplankton) are better adapted to low nutrient conditions due to larger surface to biovolume ratio.

Increased nutrient concentrations and availability of sufficient light levels possibly led to faster growth rates and increased biomass of *Synechococcus* in the southern stations along with microplankton (diatoms). Similar observation on co-occurrence of the highest biomass of picoplankton (*Synechococcus*) along with diatom abundance has been previously recorded in the north-western Arabian Sea (Tarran et al., 1999). *Prochlorococcus* is also recognized as functionally incapable to utilize nitrate in the upwelled waters unlike the microplankton and *Synechococcus* and thus, this may have resulted in decrease in its number.

In addition, low temperature of the upwelled water possibly inhibited the growth of this strain of *Prochlorococcus* (Linacre et al., 2010). Thus, contrasting physicochemical and environmental features across the north-south transect led to characteristic distribution pattern of picoplankton (*Prochlorococcus* and *Synechococcus)* during the early phase of the southwest monsoon. Upwelling, which brings nutrient-enriched subsurface waters along the west coast of India during the south-west monsoon, begins and ends a little earlier in the south than in the north. Upwelling that was at the initial phase in the southern region during the study period showed a characteristic change in autotrophs (microplankton-dominated). In contrast, the northern region was picoplankton-dominated. Such marked demarcation could lead to different ecological niches along the eastern Arabian Sea and can profoundly influence the fishery potential of the region.

5. Conclusion

The present study highlights the linkage between phytoplankton distribution and environmental parameters observed during the onset of the south-west monsoon in the Eastern Arabian Sea. The nutrient-rich upwelled waters at the south were rich in Chl *a* biomass, dominated by diatoms and picoplankton (especially *Synechococcus*), while *Prochlorococcus* were prevalent in the relatively oligotrophic northern section. Due to their spatio-temporal variability, detailed investigations are needed to address the food web structure of the region.

Acknowledgement

The authors wish to thank the Director, CSIR- NIO for his great support and encouragement. We are thankful to Mr. B. Thorat and Mr. Rasiq K.T for their support in sample collection and analysis. Dr. N.V Madhu and Mr. Ullas are acknowledged for helping in CHEMTAX analysis. Authors also wish to thank the crew members of RV *Sagar Kanya* for all the logistic support. Authors also acknowledge the editor and anonymous reviewer who helped to improve the quality of manuscript. This is NIO contribution No.

Reference

Banse, K., 1959. On upwelling and bottom-trawling off the southwest coast of India. Journal of the Marine Biological Association of India.

Banse, K., 1968. Hydrography of the Arabian Sea shelf of India and Pakistan and effects on demersal fishes. Deep-Sea Res. 15, 45-79.

Banse, K., 1987. Seasonality of phytoplankton chlorophyll in the central and northern Arabian Sea. Deep-Sea Res. 34, 713-723.

Barlow, R., Kyewalyanga, M., Sessions, H., Van den Berg, M., Morris, T., 2008. Phytoplankton pigments, functional types, and absorption properties in the Delagoa and Natal Bights of the Agulhas ecosystem. Estuar. Coast. Shelf Sci. 80, 201-211.

Barlow, R.G., Mantoura, R.F.C., Cummings, D.G., 1998. Phytoplankton pigment distributions and associated fluxes in the Bellingshausen Sea during the austral spring 1992. J. Mar. Syst. 17 (1), 97-113.

Bhattathiri, P.M.A., Pant, A., Sawant, S.S., Gauns, M., Matondkar, S.G.P., Mohanraju, R., 1996. Phytoplankton production and chlorophyll distribution in the eastern and central Arabian Sea in 1994-1995. Curr. Sci. 71, 857-862.

Brock, J.C., McClain, C.R., 1992. Interannual variability in phytoplankton blooms observed in the northwestern Arabian Sea during the southwest monsoon. J. Geophys. Res. 97, 733-750.

Brock, J.C., McClain, C.R., Luther, M.E., Hay, W.W., 1991. The phytoplankton bloom in the northwestern Arabian Sea during the southwest monsoon of 1979. J. Geophys. Res. 96, 20623-20642.

Brock, J.C., Sathyendranath, S., Platt, T., 1993. Modelling the seasonality of subsurface light and primaryproduction in the Arabian Sea. Mar. Ecol. Prog. Ser. 101, 209-221.

Brock, J.C., Sathyendranath, S., Platt, T., 1994. A model study of seasonal mixed-layer production in the Arabian Sea. P. Indian As-Earth. 103, 65-78.

Brown, S.L., Landry, M.R., Barber, T.R., Campbell, L., Garrison, L.D., Gowing, M.M., 1999. Picophytoplankton dynamics and production in the Arabian Sea during the 1995 southwest monsoon. Deep-Sea Res. 46, 1745-1768.

Buesseler, K.O., 1998. The decoupling of production and particulate export in the surface ocean. Global Biogeochem. Cycles. 12, 297-310.

Campbell, L., Liu, H., Nolla, H.A., Vaulot, D., 1997. Annual variability of phytoplankton and bacteria in the subtropical North Pacific Ocean at Station ALOHA during the 1991-1994 ENSO event. Deep-Sea Res. 44, 167-192.

Campbell, L., Landry, M.R., Constantinou, J., Nolla, H.A., Brown, S.L., Liu, H., Caron, D. A., 1998. Response of microbial community structure to environmental forcing in the Arabian Sea. Deep-Sea Res. II. 45(10-11), 2301-2325.

Casamayor, E.O., Ferrera I., Cristina X., Borrego C.M., Gasol, J.M., 2007. Flow cytometric determination of sulfide oxidation and sulfur accumulation rates by laboratory cultures and natural population of photosynthetic sulfur bacteria. Environ. Microbiol. 9, 1969-1985.

Claustre, H., 1994. The trophic status of various oceanic provinces as revealed by phytoplankton pigment signatures. Limnol. Oceanogr. 39, 1206-1210.

Cushing, D.H., 1989. A difference in structure between ecosystems in strongly stratified waters and in those that are only weakly stratified. J. Plankton Res. 11, 1-13.

Durand, M.D., Olson, R. J., Chisholm, S.W., 2001. Phytoplankton population dynamics at the Bermuda Atlantic Time-series station in the Sargasso Sea. Deep-Sea Res. II. 48(8), 1983-2003.

Falkowski, P.G., Barber, R.T., Smetacek, V., 1998. Biogeochemical controls and feedback on ocean primary production. Science. 281, 340-343.

Garrison, D.L., Gowing, M.M., Hughes, M.P., 1998. Nano and microplankton in the northern Arabian Sea during the Southwest Monsoon, August–September 1995 A US–JGOFS study. Deep-Sea Res. II. 45(10-11), 2269-2299.

Gauns, M., Mohanraju, R., Madhupratap, M., 1996. Studies on the microzooplankton from the central and eastern Arabian Sea. Curr. Sci. 71, 874-877.

Gibb, S.W., Cummings, D.G., Irigoien, X., Barlow, R.G., Fauzi, R., Mantoura, R.F.C., 2001. Phytoplankton pigment chemotaxonomy of the northeastern Atlantic. Deep-Sea Res. II. 48, 795-823.

Grasshoff, K., Erhardt, M., Kremiling, K., 1983. Methods of Seawater Analysis. Verlag Chemie, 419.

Habeebrehman, H., Prabhakaran, M.P., Jacob, J., Sabu, P., Jayalakshmi, K.J., Achuthankutty, C.T., Revichandran, C., 2008. Variability in biological responses influenced by upwelling events in the Eastern Arabian Sea. J. Mar. Syst. 74. 545-560.

Hallegraeaff, G.M., Jeffrey, S.W., 1985. Description of new chlorophyll a alteration products in marine phytoplankton. Deep-Sea Res. 32, 697-705.

Jeffrey, S.W., Vesk M., 1997. Introduction to marine phytoplankton and their pigment signatures, In: Phytoplankton pigments in oceanography: guidelines to modern methods, S.W. Jeffrey, R.F.C. Mantoura and S.W. Wright (eds.), UNESCO Publ., Paris, 37-84.

Jyothibabu, R., Madhu, N.V., Jayalakshmi, K.V., Balachandran, K.K., Shiyas, C.A., Martin G.D., Nair, K.K.C., 2006. Impact of large river influx on microzooplankton and its implications on the food web of tropical estuary (Cochin backwaters - India). Estuar. Coast. Shelf Sci. 69, 505-518.

Kleinje, A., 1991. Holococcolithophorids from the Indian Ocean, Red Sea, Mediterranean Sea and NorthAtlantic Ocean. Mar. Micropaleantol. 17, 1-76.

Knap, A.H., Michaels, A., Close, A.R., Ducklow, H., Dickson, A.G., 1996. Protocols for the joint global ocean flux study (JGOFS) core measurements. JGOFS, Reprint of the IOC Manuals and Guides No. 29, UNESCO 1994, 19.

Krey, J., 1973. Primary production in the Indian Ocean I. In:Zeitzschel, B , Gerlach, S.A. (eds.) Biology of the IndianOcean. Springer-Verlag, Berlin, 115-126.

Kurian, S., Roy, R., Repeta, D. J., Gauns, M. U., Shenoy, D. M., Suresh, T., Naqvi, S.W.A., 2012. Seasonal occurrence of anoxygenic photosynthesis in Tillari and Selaulim reservoirs, Western India. Biogeosciences. 9, 2485-2495.

Latasa, M., Bidigare, R.R., 1998. A comparison of phytoplankton populations of the Arabian Sea during the Spring Intermonsoon and Southwest Monsoon of 1995 as described by HPLC-analyzed pigments. Deep-Sea Res. II. 45(10), 2133-2170.

Linacre, L.P., Landry, M.R., Lara-Lara, J.R., Hernandez-Ayon, J.M., Bazan-Guzman, C., 2010. Picoplankton dynamics during contrasting seasonal oceanographic conditions at a coastal upwelling station off Northern Baja California, Mexico. J. Plankton Res. 32 (4), 539-557.

Mackey, M.D., Mackey, D.J., Higgins, H.W., Wright, S.W., 1996. CHEMTAX– a program for estimating class abundances from chemical markers: application to HPLC measurements of phytoplankton, Mar. Ecol. Prog. Ser. 144, 265-283.

Madhupratap, M., Prasanna kumar, S., Bhattathiri, P. M.A., Dileep kumar, M., Raghukumar, S., Nair, K.K.C., Ramaiah, N., 1996. Mechanism of the biological response to winter cooling in the northeastern Arabian Sea. Nature. 384, 549-552.

Menon, N.N., Balchand, A.N., Menon, N.R., 2000. Hydrobiology of the Cochin backwater system - a review. Hydrobiologia. 430, 149-183.

Marie, D., Partensky, F. Jacquet, S., Vaulot, D., 1997. Enumeration and cell cycle analysis of natural populations of marine picoplankton by flow cytometry using the nucleic acid stain SYBR Green I. Appl. Environ. Microbiol. 63 (1), 186-193.

Michaels, A.F., Silver, M.W., 1988. Primary production, sinking fluxes and the microbial food web. Deep-Sea Res. 3, 473-490.

Naqvi, S.W.A., Jayakumar, D.A., Narvekar, P.V., Naik, H., Sarma, V.V.S.S., D'Souza, W., Joseph, S., George, M.D., 2000. Increased marine production of N_2O due to intensifying anoxia on the Indian continental shelf. Nature. 408, 346-349.

Paerl, H.W., Valdes, L.M., Pinckney, J.L., Piehler, M.F., Dyble, J., Moisander, P.H., 2003. Phytoplankton photopigments as indicators of estuarine and coastal eutrophication. BioScience. 53(10), 953-964.

Partensky, F., Hess, W.R., Vaulot, D., 1999. Prochlorococcus, a marine photosynthetic prokaryote of global significance. Microbiol. Mol. Biol. Res. 63 (1), 106-127.

Peinert, R., von Bodungen, B., Smetacek, V.S., 1989. Food web structure and loss rate. In: Berger, W.H., Smetacek, V.S., Wefer, G. (Eds.), Productivity of the Ocean: Present and Past. Wiley, New York, 35-48.

Ramaiah, N., Raghukumar, S., Gauns, M., 1996 Bacteria abundance and production in central and eastern Arabian Sea. Curr. Sci. 71, 878-882.

Roy, S., Chanut, J., Gosselin, M., Sime-Ngando, T., 1996. Characterizationof phytoplankton communities in the lower St. Lawrence Estuary using HPLC-detected pigments and cell microscopy, Mar. Ecol. Prog. Ser. 142, 55-73.

Roy, R., Pratihary, A., Mangesh, G., Naqvi, S.W.A., 2006. Spatial variation of phytoplankton pigments along the southwest coast of India. Estuar. Coast. Shelf Sci. 69 (1), 189-195.

Sankaranarayanan, V.N., 1978. Some physical and chemical studies of the waters of the northern Arabian Sea. Ph.D. Thesis, Kerala University, Trivandrum, India.

Sawant, S.S., Madhupratap, M., 1996. Seasonality and composition of phytoplankton in the Arabian Sea. Curr. Sci. 71, 869-873.

Schluter, L., Henriksen, P., Nielsen, T.G., Jakobsen, H.H., 2011. Phytoplankton composition and biomass across the southern Indian Ocean. Deep-Sea Res. Part I. 58, 546-556.

Schluter, L., Mohlenberg, F., Havskum, H., Larsen, S., 2000. The use of phytoplankton pigments for identifying and quantifying phytoplankton groups in coastal areas: testing the influence of light and nutrients on pigment/chlorophyll a ratios. Mar. Ecol. Prog. Ser. 192, 49-63.

Shetye, S.R., Gouveia, A.D., Shenoi, S.S.C., Sundar, D., Michael, G.S., Almeida, A.M., Santanam, K. 1990. Hydrography and circulation off the west coast of India during the southwest monsoon. J. Mar. Res. 48, 359-378.

Sherr, E.B., Sherr, B.F., Wheeler, P.A., 2005. Distribution of coccoid cyanobacteria and small eukaryotic phytoplankton in the upwelling ecosystem off the Oregon coast during 2001 and 2002. Deep-Sea Res. II. 52 (1), 317-330.

Simonsen, J., 1974. Oxygen fluctuations in streams. Ph.D. Thesis, Dept. of Sanitary engineering.Technical Univ. of Denmark.

Suzuki, K., Handa, N., Nishida., T., Wong, C.S., 1997. Estimation of phytoplankton succession in a fertilized mesocosm during summer using high-performance liquid chromatographic analysis of pigments. J. Exp. Mar. Biol. Ecol. 214, 1-17.

Tarran, G.A., Burkill, P.H., Edwards, E.S., Woodward, E.M.S., 1999. Phytoplankton community structure in the Arabian Sea during and after the SW monsoon, 1994. Deep Sea Res. II: Topical Studies in Oceanography 46, 655–676. doi:10.1016/S0967-0645(98)00122-2.

Taylor, F.J.R., 1976. Dinoflagellates from the International Indian Ocean Expedition: a report on material collected by the R.V. ‘‘Anton Bruun’’ 1963-1964. Bibliotheca Botanica. 132-234.

Uitz, J., Claustre, H., Morel, A., Hooker, S. B., 2006. Vertical distribution of phytoplankton communities in Open Ocean: an assessment based on surface chlorophyll. J. Geophys. Res., 111.

Vaulot, D., Partensky, F., Neveux, J., Mantoura, R.F.C., Llewellyn, C.A., 1990. Winter presence of prochlorophytes in surface waters of the northwestern Mediterranean Sea. Limnol. Oceanogr. 35 (5), 1156-1164.

Vaulot, D., Courties, C., Partensky, F., 1989. A simple method to preserve oceanic phytoplankton for flow cytometric analyses. Cytometry. 10 (5), 629-635.

Vidussi, F., Claustre, H., Manca, B.B., Luchetta, A., Marty, J.C., 2001. Phytoplankton pigment distribution in relation to upper thermocline circulation in eastern Mediterranean Sea during winter. J. Geophys. Res. 106, 19939-19956.

Wiggert, J.D., Hood, R.R., Banse, K., Kindle J.C., 2005. Monsoon-driven biogeochemical processes in the Arabian Sea. Prog. Oceanogr. 65 (2), 176-213.

Wright, S.W., Ishikawa, A., Marchant, H.J., Davidson, A.T., van den Enden, R.L. Nash, G.V., 2009. Composition and significance of picophytoplankton in Antarctic waters. Pol. Biol. 32, 797-808.

Wright, S.W., Jeffrey, S.W., 2006. Pigment markers for phytoplankton production. Marine Organic Matter: Biomarkers, Isotopes and DNA. Springer, Berlin Heidelberg. 71-104.

Wright, S.W., Thomas, D.P., Marchant, H.J., Higgins, H.W., Mackey, M.D., Mackey, D.J., 1996. Analysis of phytoplankton of the Australian sector of the Southern Ocean: comparisons of microscopy and size frequency data with interpretations of pigment HPLC data using the CHEMTAX matrix factorisation program. Mar. Ecol. Prog. Ser. 144, 285-298.

Wright, S.W., Van den Enden, R.L., Pearce, I., Davidson, A.T., Scott, F.J., Westwood, K.J., 2010. Phytoplankton community structure and stocks in the Southern Ocean (30–80 E) determined by CHEMTAX analysis of HPLC pigment signatures. Deep-Sea Res. II. 57, 758-778.

Zwirglmaier, K., Jardillier, L., Ostrowski, M., Mazard, S., Garczarek, L., Vaulot, D., Scanlan, D. J., 2008. Global phylogeography of marine Synechococcus and Prochlorococcus reveals a distinct partitioning of lineages among oceanic biomes. Environ. Microbiol. 10 (1), 147-161.

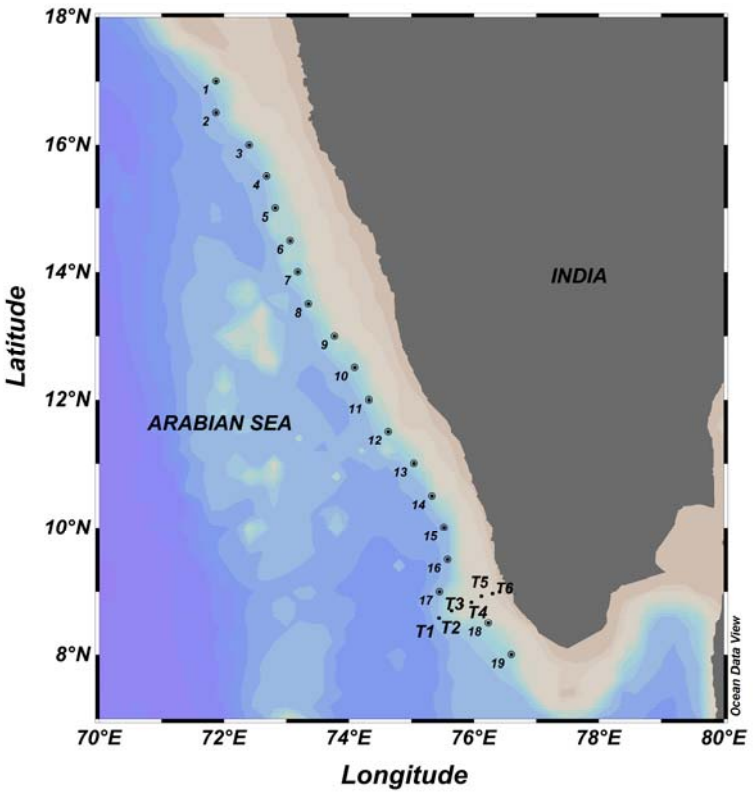

Fig. 1 Map showing station locations along the NS (1 to 19) and TVM transect (T1 to T6).

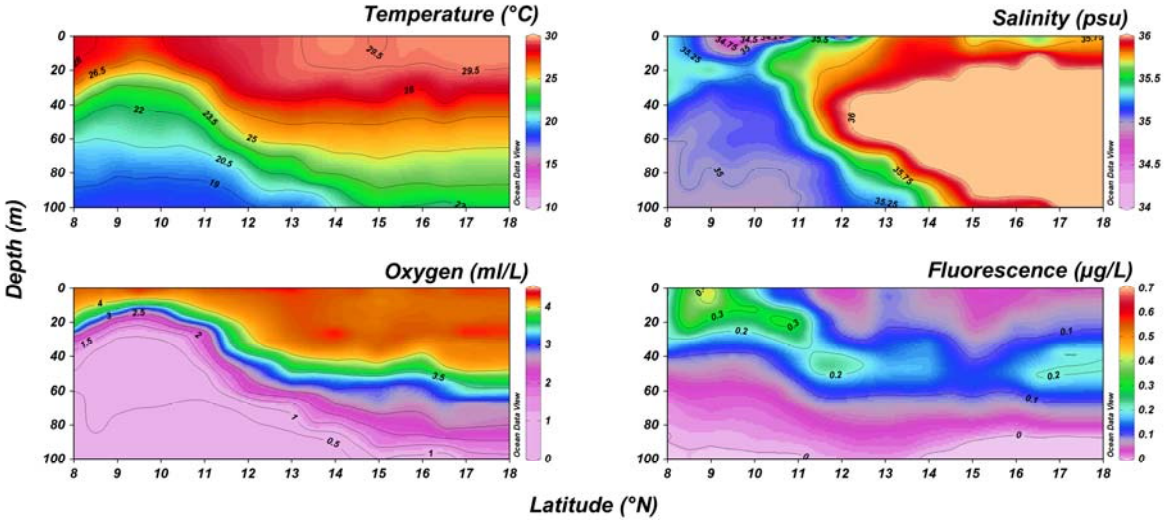

Fig. 2 Latitudinal variation of temperature, salinity, DO and Fluorescence along the Eastern Arabian Sea.

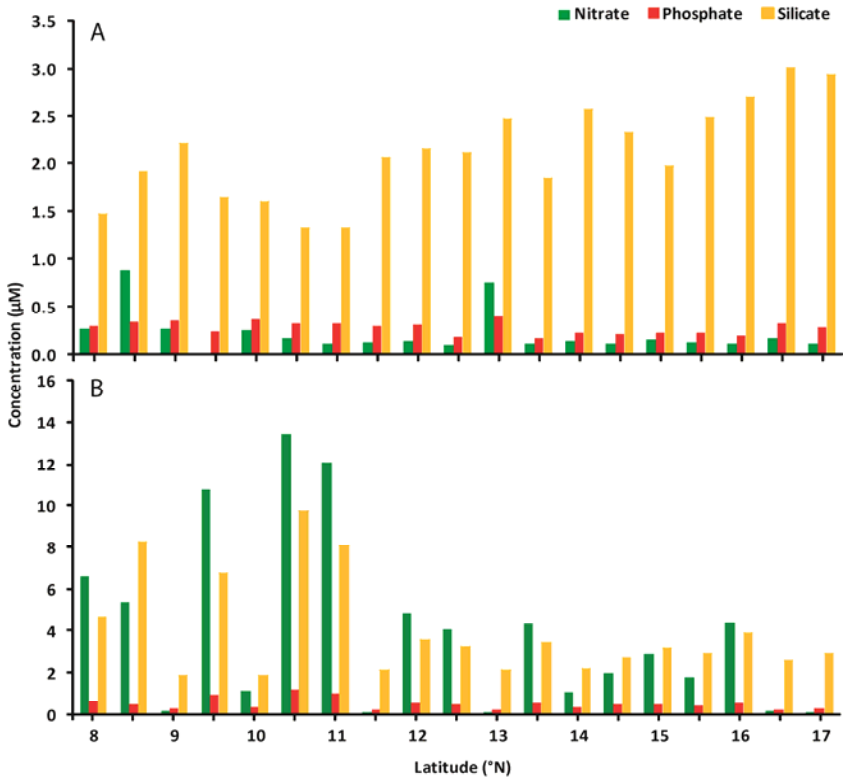

Fig. 3 Concnectration of nitrate, phosphate and silicate (µM) at (A) surface and (B) Chl_{max} along the NS transect.

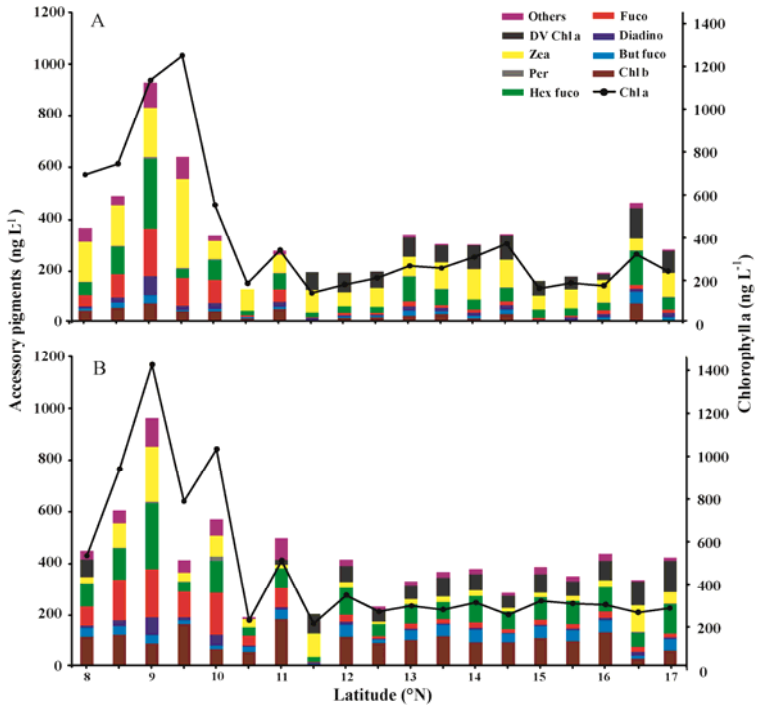

Fig. 4 Distribution of accessory pigments along the NS transect of Eastern Arabian Sea (A) surface water and (B) at Chl_{max}. The black line with dark circles represents the chlorophyll *a* concentration. Pigment abbreviations are defined in Table 1.

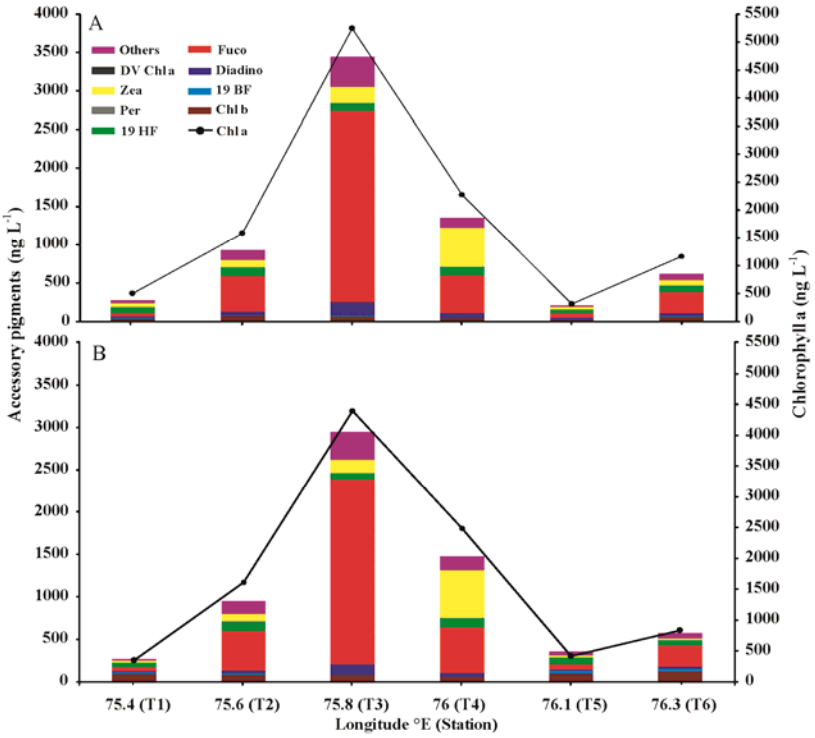

Fig. 5 Distribution of accessory pigments along TVM transect (A) in surface water and (B) at Chl_{max}. The black line with dark circles represents the chlorophyll *a* concentration.

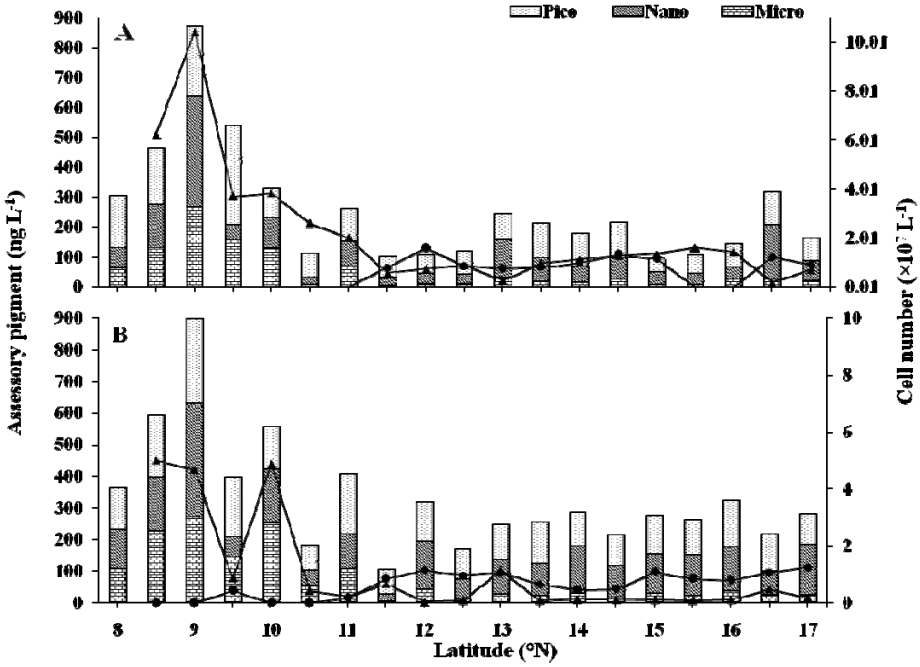

Fig. 6 Spatial variation of phytoplankton size fractions along the NS transect (A) in surface water and (B) at Chl_{max}. The black line with dark circles and triangles represents the *Prochlorococcus* and *Synechococcus* abundance respectively.

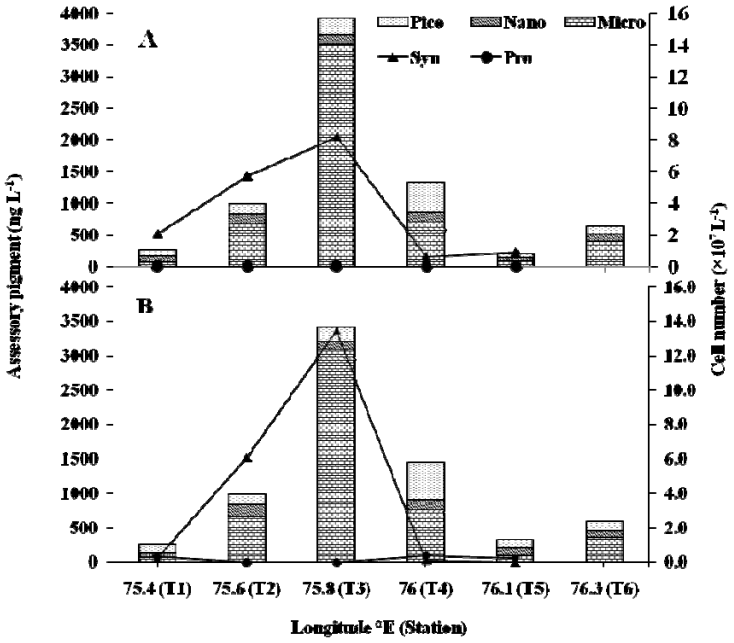

Fig. 7 Spatial variation of phytoplankton size fractions along TVM transect (A) in surface water and (B) at Chl_{max}. The black line with dark circles and triangles represents the *Prochlorococcus* and *Synechococcus* abundance respectively.

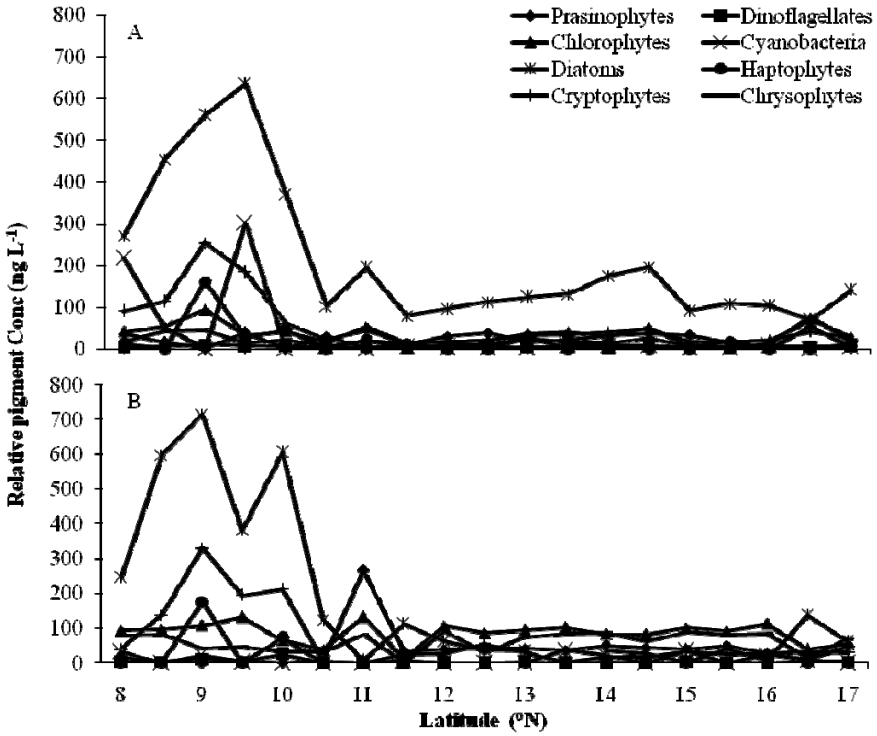

Fig. 8 CHEMTAX derived relative pigment concentration of phytoplankton groups to total Chl *a* concentration along the NS transect (A) in surface water and (B) at Chl_{max}.

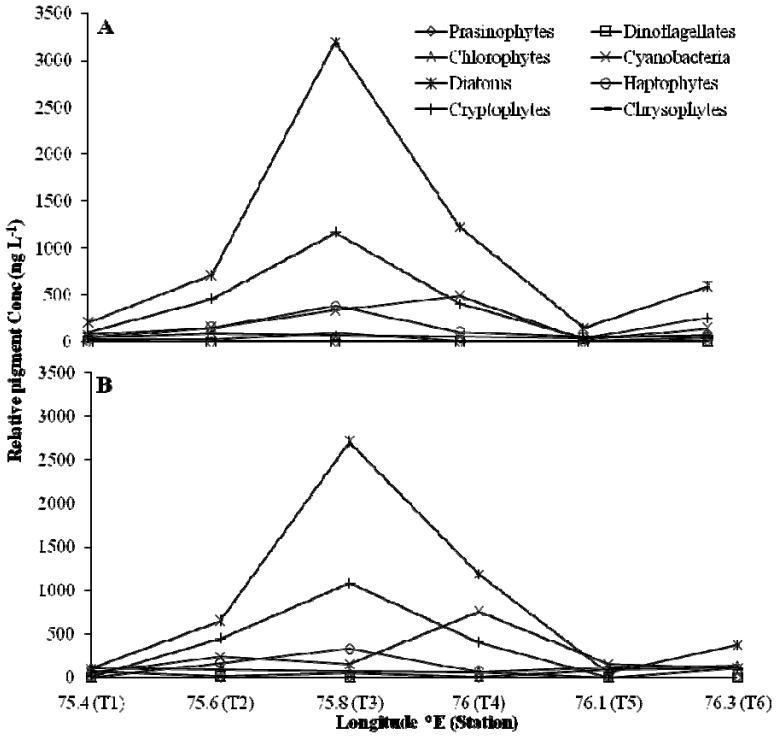

Fig. 9 CHEMTAX derived relative pigment concentration of phytoplankton groups to total Chl *a* concentration along TVM transect (A) in surface water and (B) at Chl_{max}.

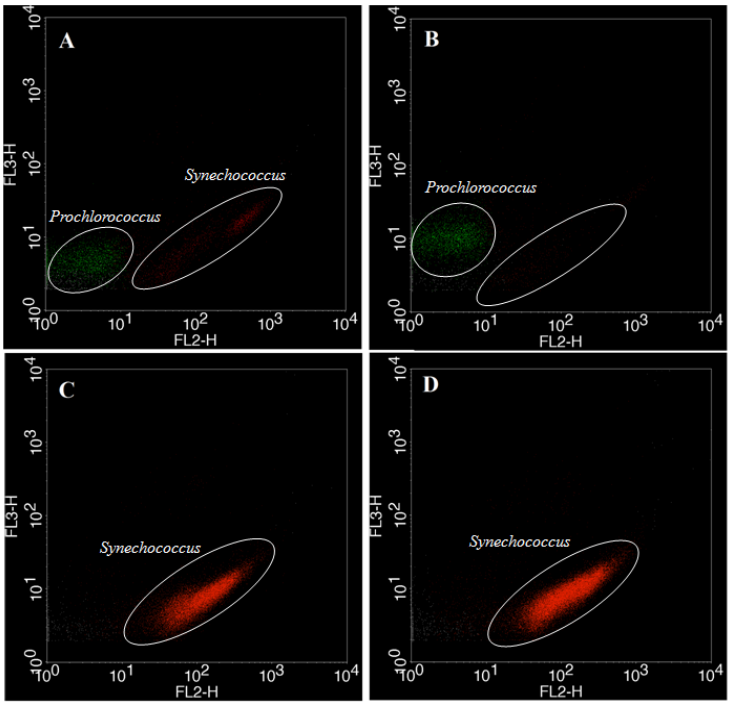

Fig. 10 Representative flow cytometer derived scatter plots from northern section (Stn. 1) (A) in surface water and (B) at Chl_{max} and southern section (Stn. T4; TVM transect), (C) in surface water and (D) at Chl_{max}. Red and green dots represent *Synechococcus* and *Prochlorococcus* cells respectively.

Table 1. Distribution of major taxonomically significant pigments in algal classes using SCOR abbreviations (Jeffrey et al., 1997).

Pigment	Abbreviation	Specificity
Chlorophyll *a*	Chl *a*	All photosynthetic algae
Chlorophyll *b*	Chl *b*	Dominant in green algae
Chlorophyll *c*2	Chl *c*2	Minor in red algae
Chlorophyll *c*3	Chl *c*3	Dominant in haptophyte, many diatoms and some dinoflagellates
β-Carotene	β-Car	Dominant in chlorophytes, prasinophytes, minor in all other algal groups
Alloxanthin	Allo	Major in Cryptophytes
19'-butanoyloxyfucoxanthin	19 BF	Dominant in pelagophytes, dictyochophytes. Present in some haptophytes
Diadinoxanthin	Diadino	Diatoms, haptophytes, pelagophytes, dictyochophytes and some dinoflagellates
Divinyl chlorophyll *a*	Div Chl *a*	Prochlorophytes
Fucoxanthin	Fuco	Diatom, Dominant in most red algae
19'-hexanoyloxyfucoxanthin	19 HF	Major in Haptophytes and dinoflagellates (lacking Peridinin)
Neoxanthin	Neo	Chlorophytes, prasinophytes
Peridinin	Peri	Dinoflagellates
Prasinoxanthin	Pras	Prasinophytes
Zeaxanthin	Zea	Dominant in cyanobacteria, pelagophytes, chrysophytes, some dinoflagellates

Table 2. Dominant phytoplankton species (×10^3 cells L^{-1}) in the northern and southern stations

	North		South					
	Station 6		Station 15		Station 17		TVM transect (T3)	
Group	**Surface**	**Chlmax**	**Surface**	**Chlmax**	**Surface**	**Chlmax**	**Surface**	**Chlmax**
Diatoms								
Amphora sp.	**0**	**0**	**0**	**0.0**	**0.43**	**0.23**	**0**	**0**
Chaetoceros coarctatus	**0**	**0**	**0**	**2.48**	**0.0**	**0**	**6.00**	**0**
Cocconeis sp.	**0**	**0**	**0**	**0.50**	**0.0**	**0**	**0.0**	**0**
Coscinodiscus sp.	**0**	**0**	**0.56**	**0.74**	**0.65**	**0**	**0.0**	**0**
Dactyliosolen fragilissimus	**0**	**0**	**0**	**0**	**0.00**	**0**	**199.33**	**550.25**
Guinardia striata	**0**	**0**	**0**	**0**	**1.51**	**0**	**0.0**	**0**
Leptocylindrus danicus	**0**	**0**	**0**	**0**	**0.0**	**0**	**18.67**	**0**
Navicula sp.	**0**	**0**	**0**	**0**	**1.73**	**0**	**0.67**	**1.55**
Nitzschia sp.	**0**	**0.38**	**0**	**0**	**0**	**0**	**0**	**3.10**
Pseudo-nitzschia heimii	**0**	**0**	**0**	**0**	**0**	**0**	**6.00**	**0**
Rhizosolenia curvata	**0**	**0**	**0**	**0.25**	**0**	**0**	**0**	**0**
Rhizosolenia imbricata	**0**	**0**	**0**	**0.0**	**0**	**0**	**4.00**	**1.55**
Rhizosolenia sp.	**0**	**0**	**0**	**0.25**	**0**	**0**	**0**	**0**
Thalassiosira sp.	**1.34**	**0.58**	**6.16**	**6.45**	**2.81**	**1.39**	**2.00**	**0**
Dinoflagellates								
Ceratium sp.	**0**	**0.19**	**0**	**0**	**0.0**	**0**	**0**	**0**
Gonyaulax hyalina	**0**	**0**	**0**	**0**	**0.22**	**0**	**0**	**0**
Gonyaulax polyedra	**0**	**0.19**	**0**	**0**	**0**	**0**	**0**	**0**
Gyrodinium sp.	**0.22**	**0**	**0**	**0.50**	**0**	**0**	**0**	**0**
Ornithocercus sp.	**0.22**	**0**	**0**	**0**	**0**	**0**	**0**	**0**
Oxytoxum laticeps	**0.22**	**0**	**0**	**0**	**0**	**0**	**0**	**0**
Oxytoxum nanum	**0.90**	**0**	**0**	**0**	**0**	**0**	**0**	**0**
Oxytoxum parvum	**0**	**0**	**0**	**0.25**	**0**	**0**	**0**	**0**
Oxytoxum sp.	**0**	**0.38**	**0**	**0.0**	**0**	**0**	**0**	**0**
Oxytoxum viride	**0**	**0**	**0**	**0.25**	**0**	**0**	**0**	**0**
Prorocentrum micans	**0**	**0**	**0**	**0.25**	**0**	**0**	**0**	**0**
Protoperidinium sp.	**0.22**	**0**	**0**	**0.0**	**0**	**0**	**0**	**0**
Scrippsiella sp.	**0.90**	**0.19**	**0**	**0.74**	**1.08**	**0.46**	**0**	**0**

SUPPLEMENTARY TABLES

Table S1.A. Marker pigments to Chl *a* ratios. Input ratios were obtained from literature.

Groups	Chl c3	Chl c2	Peri	19 BF	Fuco	Neo	Pras	19 HF	Diadino	Allo	Zea	Chl b	b-Car
NS													
Prasinophytes	0	0	0	0	0	0.034	0.043	0	0	0	0.006	0.009	0.047
Dinoflagellates	0	0.017	0.483	0	0	0	0	0	0.045	0	0	0	0
Chlorophytes	0	0	0	0	0	0.015	0	0	0.241	0	0	0.569	0
Cyanobacteria	0	0	0	0	0	0	0	0	0	0	0.048	0	0.139
Diatoms	0	0	0	0	0.159	0	0	0	0.03	0	0	0	0
Haptophytes	0.097	0	0	0.023	0.08	0	0	0.01	0.06	0	0	0	0.02
Cryptophytes	0	0.077	0	0	0	0	0	0	0	0.042	0	0	0
Chrysophytes	0.125	0.127	0	0.303	0.275	0.013	0	0	0.018	0	0	0	0.016
Off TVM													
Dinoflagellates	0	0.017	0.483	0	0	0	0	0	0.045	0	0	0	0
Chlorophytes	0	0	0	0	0	0	0	0	0.241	0	0	0.569	0
Cyanobacteria	0	0	0	0	0	0	0	0	0	0	0.048	0	0.139
Diatoms	0	0	0	0	0.159	0	0	0	0.03	0	0	0	0
Haptophytes	0.097	0	0	0.023	0.08	0	0	0.01	0.06	0	0	0	0.02
Cryptophytes	0	0.077	0	0	0	0	0	0	0	0.042	0	0	0
Chrysophytes	0.125	0.127	0	0.303	0.275	0	0	0	0.018	0	0	0	0.016

Table S1.B. Estimated output ratios based on CHEMTAX program.

Groups	Chl c3	Chl c2	Peri	19 BF	Fuco	Neo	Pras	19 HF	Diadino	Allo	Zea	Chl b	b-Car
NS													
Prasinophytes	0	0	0	0	0	0.030	0.038	0	0	0	0.005	0.008	0.041
Dinoflagellates	0	0.011	0.313	0	0	0	0	0	0.029	0	0	0	0
Chlorophytes	0	0	0	0	0	0.008	0	0	0.066	0	0	0.381	0
Cyanobacteria	0	0	0	0	0	0	0	0	0	0	0.040	0	0.117
Diatoms	0	0	0	0	0.120	0	0	0	0.023	0	0	0	0
Haptophytes	0.075	0	0	0.018	0.062	0	0	0.008	0.047	0	0	0	0.016
Cryptophytes	0	0.069	0	0	0	0	0	0	0	0.038	0	0	0
Chrysophytes	0.065	0.049	0	0.195	0.144	0.007	0	0	0.009	0	0	0	0.008
Off TVM													
Dinoflagellates	0	0.011	0.313	0	0	0	0	0	0.029	0	0	0	0
Chlorophytes	0	0	0	0	0	0	0	0	0.067	0	0	0.391	0
Cyanobacteria	0	0	0	0	0	0	0	0	0	0	0.046	0	0.095
Diatoms	0	0	0	0	0.153	0	0	0	0.022	0	0	0	0
Haptophytes	0.075	0	0	0.018	0.062	0	0	0.008	0.047	0	0	0	0.016
Cryptophytes	0	0.069	0	0	0	0	0	0	0	0.038	0	0	0
Chrysophytes	0.067	0.068	0	0.163	0.148	0	0	0	0.010	0	0	0	0.009